A Joint Search for Gravitational Wave Bursts with AURIGA and LIGO

L. Baggio[47], M. Bignotto[48], M. Bonaldi[49], M. Camarda[50] , M. Cerdonio[*48], L. Conti[48], M. De Rosa[51], P. Falferi[49], S. Fattori[48], P. Fortini[52], M. Inguscio[53], N. Liguori[48], S. Longo[48] , F. Marin[53], R. Mezzena[54], A. Mion[54], A. Ortolan[56], S. Poggi[55], G.A. Prodi[54], F. Salemi[54], G. Soranzo[57], L. Taffarello[57], G. Vedovato[57], A. Vinante[49], S. Vitale[54], J.P. Zendri[57]

(AURIGA collaboration, provisional list to be confirmed)
47 ...
[48]8INFN Padova Section and Department of Physics, University of Padova, I-35131 Padova, Italy
[49] Istituto di Fotonica e Nanotecnologie CNR-ITC and INFN Gruppo Collegato di Trento, Padova Section, I-38050 Povo (Trento), Italy
[50] Dipartimento di Ingegneria dell'Informazione, University of Padova, I-35131 Padova, Italy
[51] INOA I-80078 Pozzuoli (Napoli), Italy and INFN Firenze Section, I-50121 Firenze, Italy
[52] Physics Department, University of Ferrara and INFN Ferrara Section, I-44100 Ferrara, Italy
[53] LENS and Physics Department, University of Firenze and INFN Firenze Section, I-50121 Firenze, Italy
[54] Physics Department, University of Trento and INFN Gruppo Collegato di Trento, Padova Section, I-38050 Povo (Trento), Italy
[55] Consorzio Criospazio Ricerche, I-38050 Povo (Trento), Italy
[56]INFN, Laboratori Nazionali di Legnaro, I-35020 Legnaro (Padova) Italy
[57] INFN Padova Section, I-35100 Padova, Italy

B. Abbott[15], R. Abbott[15], R. Adhikari[15], J. Agresti[15], P. Ajith[2], B. Allen[2, 52], R. Amin[19], S. B. Anderson[15], W. G. Anderson[52], M. Arain[40], M. Araya[15], H. Armandula[15], M. Ashley[4], S. Aston[39], P. Aufmuth[37], C. Aulbert[1], S. Babak[1], S. Ballmer[15], H. Bantilan[9], B. C. Barish[15], C. Barker[16], D. Barker[16], B. Barr[41], P. Barriga[51], M. A. Barton[41], K. Bayer[18], K. Belczynski[25], J. Betzwieser[18], P. T. Beyersdorf[28], B. Bhawal[15], I. A. Bilenko[22], G. Billingsley[15], R. Biswas[52], E. Black[15], K. Blackburn[15], L. Blackburn[18], D. Blair[51], B. Bland[16], J. Bogenstahl[41], L. Bogue[17], R. Bork[15], V. Boschi[15], S. Bose[54], P. R. Brady[52], V. B. Braginsky[22], J. E. Brau[44], M. Brinkmann[2], A. Brooks[38], D. A. Brown[15, 7], A. Bullington[31], A. Bunkowski[2], A. Buonanno[42], O. Burmeister[2], D. Busby[15], W. E. Butler[45], R. L. Byer[31], L. Cadonati[18], G. Cagnoli[41], J. B. Camp[23], J. Cannizzo[23],

K. Cannon[52], C. A. Cantley[41], J. Cao[18], L. Cardenas[15], K. Carter[17], M. M. Casey[41], G. Castaldi[47], C. Cepeda[15], E. Chalkey[41], P. Charlton[10], S. Chatterji[15], S. Chelkowski[2], Y. Chen[1], F. Chiadini[46], D. Chin[43], E. Chin[51], J. Chow[4], N. Christensen[9], J. Clark[41], P. Cochrane[2], T. Cokelaer[8], C. N. Colacino[39], R. Coldwell[40], R. Conte[46], D. Cook[16], T. Corbitt[18], D. Coward[51], D. Coyne[15], J. D. E. Creighton[52], T. D. Creighton[15], R. P. Croce[47], D. R. M. Crooks[41], A. M. Cruise[39], A. Cumming[41], J. Dalrymple[32], E. D'Ambrosio[15], K. Danzmann[37, 2], G. Davies[8], D. DeBra[31], J. Degallaix[51], M. Degree[31], T. Demma[47], V. Dergachev[43], S. Desai[33], R. DeSalvo[15], S. Dhurandhar[14], M. Díaz[34], J. Dickson[4], A. Di Credico[32], G. Diederichs[37], A. Dietz[8], E. E. Doomes[30], R. W. P. Drever[5], J.-C. Dumas[51], R. J. Dupuis[15], J. G. Dwyer[11], P. Ehrens[15], E. Espinoza[15], T. Etzel[15], M. Evans[15], T. Evans[17], S. Fairhurst[8, 15], Y. Fan[51], D. Fazi[15], M. M. Fejer[31], L. S. Finn[33], V. Fiumara[46], N. Fotopoulos[52], A. Franzen[37], K. Y. Franzen[40], A. Freise[39], R. Frey[44], T. Fricke[45], P. Fritschel[18], V. V. Frolov[17], M. Fyffe[17], V. Galdi[47], K. S. Ganezer[6], J. Garofoli[16], I. Gholami[1], J. A. Giaime[17, 19], S. Giampanis[45], K. D. Giardina[17], K. Goda[18], E. Goetz[43], L. Goggin[15], G. González[19], S. Gossler[4], A. Grant[41], S. Gras[51], C. Gray[16], M. Gray[4], J. Greenhalgh[27], A. M. Gretarsson[12], R. Grosso[34], H. Grote[2], S. Grunewald[1], M. Guenther[16], R. Gustafson[43], B. Hage[37], D. Hammer[52], C. Hanna[19], J. Hanson[17], J. Harms[2], G. Harry[18], E. Harstad[44], T. Hayler[27], J. Heefner[15], I. S. Heng[41], A. Heptonstall[41], M. Heurs[2], M. Hewitson[2], S. Hild[37], E. Hirose[32], D. Hoak[17], D. Hosken[38], J. Hough[41], E. Howell[51], D. Hoyland[39], S. H. Huttner[41], D. Ingram[16], E. Innerhofer[18], M. Ito[44], Y. Itoh[52], A. Ivanov[15], D. Jackrel[31], B. Johnson[16], W. W. Johnson[19], D. I. Jones[48], G. Jones[8], R. Jones[41], L. Ju[51], P. Kalmus[11], V. Kalogera[25], D. Kasprzyk[39], E. Katsavounidis[18], K. Kawabe[16], S. Kawamura[24], F. Kawazoe[24], W. Kells[15], D. G. Keppel[15], F. Ya. Khalili[22], C. Kim[25], P. King[15], J. S. Kissel[19], S. Klimenko[40], K. Kokeyama[24], V. Kondrashov[15], R. K. Kopparapu[19], D. Kozak[15], B. Krishnan[1], P. Kwee[37], P. K. Lam[4], M. Landry[16], B. Lantz[31], A. Lazzarini[15], B. Lee[51], M. Lei[15], J. Leiner[54], V. Leonhardt[24], I. Leonor[44], K. Libbrecht[15], P. Lindquist[15], N. A. Lockerbie[49], M. Longo[46], M. Lormand[17], M. Lubinski[16], H. Lück[37, 2], B. Machenschalk[1], M. MacInnis[18], M. Mageswaran[15], K. Mailand[15], M. Malec[37], V. Mandic[15], S. Marano[46], S. Márka[11], J. Markowitz[18], E. Maros[15], I. Martin[41], J. N. Marx[15], K. Mason[18], L. Matone[11], V. Matta[46], N. Mavalvala[18], R. McCarthy[16], D. E. McClelland[4],

S. C. McGuire[30], M. McHugh[21], K. McKenzie[4], J. W. C. McNabb[33], S. McWilliams[23], T. Meier[37], A. Melissinos[45], G. Mendell[16], R. A. Mercer[40], S. Meshkov[15], E. Messaritaki[15], C. J. Messenger[41], D. Meyers[15], E. Mikhailov[18], S. Mitra[14], V. P. Mitrofanov[22], G. Mitselmakher[40], R. Mittleman[18], O. Miyakawa[15], S. Mohanty[34], G. Moreno[16], K. Mossavi[2], C. MowLowry[4], A. Moylan[4], D. Mudge[38], G. Mueller[40], S. Mukherjee[34], H. Müller-Ebhardt[2], J. Munch[38], P. Murray[41], E. Myers[16], J. Myers[16], T. Nash[15], G. Newton[41], A. Nishizawa[24], F. Nocera[15], K. Numata[23], B. O'Reilly[17], R. O'Shaughnessy[25], D. J. Ottaway[18], H. Overmier[17], B. J. Owen[33], Y. Pan[42], M. A. Papa[1, 52], V. Parameshwaraiah[16], C. Parameswariah[17], P. Patel[15], M. Pedraza[15], S. Penn[13], V. Pierro[47], I. M. Pinto[47], M. Pitkin[41], H. Pletsch[2], M. V. Plissi[41], F. Postiglione[46], R. Prix[1], V. Quetschke[40], F. Raab[16], D. Rabeling[4], H. Radkins[16], R. Rahkola[44], N. Rainer[2], M. Rakhmanov[33], M. Ramsunder[33], K. Rawlins[18], S. Ray-Majumder[52], V. Re[39], T. Regimbau[8], H. Rehbein[2], S. Reid[41], D. H. Reitze[40], L. Ribichini[2], R. Riesen[17], K. Riles[43], B. Rivera[16], N. A. Robertson[15, 41], C. Robinson[8], E. L. Robinson[39], S. Roddy[17], A. Rodriguez[19], A. M. Rogan[54], J. Rollins[11], J. D. Romano[8], J. Romie[17], R. Route[31], S. Rowan[41], A. Rüdiger[2], L. Ruet[18], P. Russell[15], K. Ryan[16], S. Sakata[24], M. Samidi[15], L. Sancho de la Jordana[36], V. Sandberg[16], G. H. Sanders[15], V. Sannibale[15], S. Saraf[26], P. Sarin[18], B. S. Sathyaprakash[8], S. Sato[24], P. R. Saulson[32], R. Savage[16], P. Savov[7], A. Sazonov[40], S. Schediwy[51], R. Schilling[2], R. Schnabel[2], R. Schofield[44], B. F. Schutz[1, 8], P. Schwinberg[16], S. M. Scott[4], A. C. Searle[4], B. Sears[15], F. Seifert[2], D. Sellers[17], A. S. Sengupta[8], P. Shawhan[42], D. H. Shoemaker[18], A. Sibley[17], J. A. Sidles[50], X. Siemens[15, 7], D. Sigg[16], S. Sinha[31], A. M. Sintes[36, 1], B. J. J. Slagmolen[4], J. Slutsky[19], J. R. Smith[2], M. R. Smith[15], K. Somiya[2, 1], K. A. Strain[41], D. M. Strom[44], A. Stuver[33], T. Z. Summerscales[3], K.-X. Sun[31], M. Sung[19], P. J. Sutton[15], H. Takahashi[1], D. B. Tanner[40], M. Tarallo[15], R. Taylor[15], R. Taylor[41], J. Thacker[17], K. A. Thorne[33], K. S. Thorne[7], A. Thüring[37], K. V. Tokmakov[41], C. Torres[34], C. Torrie[41], G. Traylor[17], M. Trias[36], W. Tyler[15], D. Ugolini[35], C. Ungarelli[39], K. Urbanek[31], H. Vahlbruch[37], M. Vallisneri[7], C. Van Den Broeck[8], M. van Putten[18], M. Varvella[15], S. Vass[15], A. Vecchio[39], J. Veitch[41], P. Veitch[38], A. Villar[15], C. Vorvick[16], S. P. Vyachanin[22], S. J. Waldman[15], L. Wallace[15], H. Ward[41], R. Ward[15], K. Watts[17], D. Webber[15], A. Weidner[2], M. Weinert[2], A. Weinstein[15],

R. Weiss[18], S. Wen[19], K. Wette[4], J. T. Whelan[1], D. M. Whitbeck[33], S. E. Whitcomb[15], B. F. Whiting[40], S. Wiley[6], C. Wilkinson[16], P. A. Willems[15], L. Williams[40], B. Willke[37, 2], I. Wilmut[27], W. Winkler[2], C. C. Wipf[18], S. Wise[40], A. G. Wiseman[52], G. Woan[41], D. Woods[52], R. Wooley[17], J. Worden[16], W. Wu[40], I. Yakushin[17], H. Yamamoto[15], Z. Yan[51], S. Yoshida[29], N. Yunes[33], M. Zanolin[18], J. Zhang[43], L. Zhang[15], C. Zhao[51], N. Zotov[20], M. Zucker[18], H. zur Mühlen[37], J. Zweizig[15]

The LIGO Scientific Collaboration, http://www.ligo.org

[1] Albert-Einstein-Institut, Max-Planck-Institut für Gravitationsphysik, D-14476 Golm, Germany

[2] Albert-Einstein-Institut, Max-Planck-Institut für Gravitationsphysik, D-30167 Hannover, Germany

[3] Andrews University, Berrien Springs, MI 49104 USA

[4] Australian National University, Canberra, 0200, Australia

[5] California Institute of Technology, Pasadena, CA 91125, USA

[6] California State University Dominguez Hills, Carson, CA 90747, USA

[7] Caltech-CaRT, Pasadena, CA 91125, USA

[8] Cardiff University, Cardiff, CF24 3AA, United Kingdom

[9] Carleton College, Northfield, MN 55057, USA

[10] Charles Sturt University, Wagga Wagga, NSW 2678, Australia

[11] Columbia University, New York, NY 10027, USA

[12] Embry-Riddle Aeronautical University, Prescott, AZ 86301 USA

[13] Hobart and William Smith Colleges, Geneva, NY 14456, USA

[14] Inter-University Centre for Astronomy and Astrophysics, Pune - 411007, India

[15] LIGO - California Institute of Technology, Pasadena, CA 91125, USA

[16] LIGO Hanford Observatory, Richland, WA 99352, USA

[17] LIGO Livingston Observatory, Livingston, LA 70754, USA

[18] LIGO - Massachusetts Institute of Technology, Cambridge, MA 02139, USA

[19] Louisiana State University, Baton Rouge, LA 70803, USA

[20] Louisiana Tech University, Ruston, LA 71272, USA

[21] Loyola University, New Orleans, LA 70118, USA

[22] Moscow State University, Moscow, 119992, Russia

[23] NASA/Goddard Space Flight Center, Greenbelt, MD 20771, USA

[24] National Astronomical Observatory of Japan, Tokyo 181-8588, Japan

[25] Northwestern University, Evanston, IL 60208, USA

[26] Rochester Institute of Technology, Rochester, NY 14623, USA

[27] Rutherford Appleton Laboratory, Chilton, Didcot, Oxon OX11 0QX United Kingdom

[28] San Jose State University, San Jose, CA 95192, USA

[29] Southeastern Louisiana University, Hammond, LA 70402, USA

[30] Southern University and A&M College, Baton Rouge, LA 70813, USA

[31] Stanford University, Stanford, CA 94305, USA

[32] Syracuse University, Syracuse, NY 13244, USA

[33] The Pennsylvania State University, University Park, PA 16802, USA

[34] The University of Texas at Brownsville and Texas Southmost College, Brownsville, TX 78520, USA

[35] Trinity University, San Antonio, TX 78212, USA

[36] Universitat de les Illes Balears, E-07122 Palma de Mallorca, Spain

[37] Universität Hannover, D-30167 Hannover, Germany

[38] University of Adelaide, Adelaide, SA 5005, Australia

[39] University of Birmingham, Birmingham, B15 2TT, United Kingdom

[40] University of Florida, Gainesville, FL 32611, USA

[41] University of Glasgow, Glasgow, G12 8QQ, United Kingdom

[42] University of Maryland, College Park, MD 20742 USA

[43] University of Michigan, Ann Arbor, MI 48109, USA

[44] University of Oregon, Eugene, OR 97403, USA

[45] University of Rochester, Rochester, NY 14627, USA

[46] University of Salerno, 84084 Fisciano (Salerno), Italy
[47] University of Sannio at Benevento, I-82100 Benevento, Italy
[48] University of Southampton, Southampton, SO17 1BJ, United Kingdom
[49] University of Strathclyde, Glasgow, G1 1XQ, United Kingdom
[50] University of Washington, Seattle, WA, 98195
[51] University of Western Australia, Crawley, WA 6009, Australia
[52] University of Wisconsin-Milwaukee, Milwaukee, WI 53201, USA
[53] Vassar College, Poughkeepsie, NY 12604
[54] Washington State University, Pullman, WA 99164, USA

Abstract.
The first simultaneous operation of the AURIGA detector and the LIGO observatory was an opportunity to explore on real data joint analysis methods between two very different types of gravitational wave detectors: resonant bars and interferometers. This paper describes one implementation of coincident gravitational wave burst search, where data from the LIGO interferometers are cross-correlated at the time of AURIGA candidate events to identify coherent transients. The analysis pipeline is tuned with two thresholds, on the signal-to-noise ratio of AURIGA candidate events and on the significance of the cross-correlation test in LIGO. The false alarm rate is estimated by introducing time shifts between data sets and the network detection efficiency is measured with simulated signals with power in the narrower AURIGA band. In the absence of a detection, we discuss how to set an upper limit on the rate of gravitational waves and to interpret it according to different source models. Due to the short amount of analyzed data and to the high rate of non-Gaussian transients in the detectors noise at the time, the relevance of this study is methodological: this has been the first joint search for gravitational wave bursts among detectors with such different spectral sensitivity and the first opportunity for the resonant and interferometric communities to unify languages and techniques in the pursuit of their common goal.

1. Introduction

Gravitational wave bursts are short duration perturbations of the space-time metric due to such catastrophic astrophysical events as supernova core collapses [1] or the merger and ringdown phases of binary black hole convalescences [2, 3]. Over the past decade, the search for these signals has been independently performed by individual detectors or by homogeneous networks of resonant bars [4] or laser interferometers [6, 7, 8, 10]. The first coincident burst analysis between interferometers with different broadband sensitivity and orientation was performed by the TAMA and LIGO Scientific Collaborations [11]. That analysis required coincident detection of power excesses in at least two LIGO interferometers and in the TAMA detector in the 700-2000 Hz frequency band, where all sensitivities were comparable. The upper limit result accounted for the different antenna patterns with a Monte Carlo estimate of detection efficiency for sources uniformly distributed in the sky.

This paper describes a joint burst search in a more heterogeneous network, comprised of LIGO and AURIGA. LIGO consists of three interferometers, two co-located in Hanford, WA, with 2 km and 4 km baselines and one in Livingston, LA, with a 4 km baseline, sensitive between 60 and 4000 Hz with best performance in a 100 Hz band around 150 Hz. AURIGA is a bar detector equipped with a capacitive resonant transducer, located in Legnaro (PD), Italy. In 2003 the AURIGA detector resumed data acquisition after upgrades that enlarged its sensitive band to 850-950 Hz, from the $\sim$2 Hz bandwidth of the 1997-1999 run [12, 13, 14].

Due to the different spectral shapes, an interferometer-bar coincident search is only sensitive to signals with power in the bar's narrower band. The LIGO-AURIGA analysis thus focused on short duration ($\leq$20 ms) transients in the 850-950 Hz band, with potential target sources like black hole ringdowns [2] and binary black hole mergers [15, 16].

Another important difference between bars and interferometers is the sky coverage, which depends on the detectors' shape and orientation. Figure 1 shows the antenna pattern magnitude $\sqrt{F_+^2 + F_\times^2}$ of the AURIGA and LIGO-Hanford (LHO)

detectors, as a function of latitude and longitude. Since directions of maximum LIGO sensitivity overlap with the larger portion of the sky visible to AURIGA, a coincident search is not penalized by differences in antenna pattern. However, adding AURIGA to the detector network does not improve its overall sky coverage either, due to the 3:1 ratio in amplitude sensitivity between AURIGA and LIGO [17, 18].

Despite the different sensitivity and bandwidth, a coincident analysis between LIGO and AURIGA has the potential to suppress false alarms in the LIGO network, increasing the confidence in the detection of loud signals and making source localization possible, with triangulation. Collaborative searches also increase the amount of observation time with three or more operating detectors. For this reason, and to bring together the expertise of two traditions in burst analysis, the AURIGA and LIGO collaborations pursued a joint search.

The analysis described in this paper follows the all-sky approach described in [18], where data from two or three LIGO interferometers is cross-correlated at the time of AURIGA candidate events. This method was tested on data from the first AURIGA and LIGO coincident run, a 389 hour period between December 24, 2003 and January 9, 2004, during the third LIGO science run S3 [8] and the first run of the upgraded AURIGA detector [13, 14]. Only a portion of this data was used in the joint burst search, because of the detectors' duty factors and the selection of validated data segments which was independently performed by the two collaborations [17, 19]. The effective livetime available for the analysis was:

- 36 hours of 4-fold coincidence between AURIGA and the three LIGO interferometers;
- 74 hours of 3-fold coincidence between AURIGA and the two LIGO Hanford interferometers, when data from the LIGO Livingston detector was not available.

Other three-detector combinations including AURIGA were not considered, due to the low duty factor of the LIGO Livingston interferometer in S3. The 4-fold and 3-fold data sets were separately analyzed and the outcome was combined in a single result.

Figure 2 shows the best single-sided sensitivity spectra for LIGO and AURIGA in the 800-1000 Hz band at the time of the coincident run. The AURIGA spectrum contained spurious lines, due to the up-conversion of low frequency seismic noise. These lines were non stationary and could not always be filtered by the AURIGA data analysis; for this reason, a large portion of the data (up to 42%) had to be excluded from the analysis, with significant impact on the livetime [17, 19]. The largest peak in each LIGO spectrum is a calibration line, filtered in the analysis. The amount of available LIGO livetime was limited by several data quality factors, such as data acquisition problems, excessive dust at the optical tables, and fluctuations of the light stored in the cavities, as described in [8].

Due to the short duration of the coincidence run and the non-optimal detector performances, the work described in this paper has a methodological relevance. On the other hand, it is worth pointing out that the three-fold coincidence between AURIGA and the two Hanford interferometers, when Livingston was offline, allowed the exploration of some data that would not have been searched otherwise.

2. The analysis pipeline

The joint analysis followed a statistically *blind* procedure to avoid biases on the result: the pipeline was tested, thresholds were fixed and procedural decisions were made

before the actual search, according to the following protocol [18, 19].

(i) AURIGA provided a list of burst candidates (triggers) in the validated observation time. The triggers were identified by matched filtering to a δ-like signal, with signal-to-noise threshold SNR$\geq$ 4.5. Triggers at lower SNR were not included in this analysis, since their rate and time uncertainty increased steeply to unmanageable levels, with negligible improvement in detection efficiency. Special attention was required, in this run, to address non-stationary noise with data quality vetoes (not needed in subsequent runs) [17, 19]. The resulting events were auto-correlated up to about 300 s; this effect, particularly evident for high SNR events, was due to an imperfect suppression of the non-stationary spurious lines on short time scales.

(ii) Data from the three LIGO interferometers at the time of AURIGA triggers was cross-correlated by the r-statistic waveform consistency test [20], a component of the LIGO burst analysis [7, 8] performed with the *CorrPower* code [21]. The test compares the broadband linear cross-correlation r between two data streams to the normal distribution expected for uncorrelated data and computes its p-value, the probability of getting a larger r if no correlation is present, expressed as $\Gamma = -\mathrm{Log}_{10}(\text{p-value})$. When more than two streams are involved, Γ is the arithmetic mean of the values for each pair. The cross-correlation was performed on 20, 50 and 100 ms integration windows, to allow for different signal durations. Since the source direction was unknown, the integration windows were slid around each AURIGA trigger by 27 ms$+\sigma_t$, sum of the light travel time between AURIGA and Hanford and of the estimated 1σ timing error of the AURIGA trigger. The value of σ_t depended on the SNR of each trigger, typically in the $5-40$ ms range, with an average value of 17 ms. The resulting Γ was the maximum amongst all time slides and integration windows. Only triggers above the minimal analysis threshold of $\Gamma \geq 4$ were considered as coincidences.

(iii) A cut was applied on sign of the correlation between the two Hanford interferometers, which must be positive for a gravitational wave signal in the two co-located detectors. This cut, also used in the LIGO-only analysis [8], reduced by a factor $\sim$2 the number of accidental coincidences, with no effect on the detection efficiency.

(iv) The data analysis pipeline was first applied, for testing purposes, to a *playground* data set [22], which amounted to about 10% of the livetime and was later excluded from the data set used in the analysis.

(v) The false alarm statistics were estimated on *off-source* data sets obtained by time shifting the LIGO data; more details are provided in section 2.1.

(vi) The detection efficiency was estimated with Monte Carlo methods [19], by simulating a population of sources uniformly distributed in the sky and in polarization angle, as described in section 2.2.

(vii) The analysis tuning consisted of setting two thresholds: on the SNR of the AURIGA candidate events and on the LIGO Γ value. Details on the tuning procedure are available in section 2.3.

(viii) The statistical analysis plan was defined *a priori*, with decisions on which combination of detectors to analyze (4-fold and 3-fold) and how to merge the results, the confidence level for the null hypothesis test, and the procedure to build the confidence belt, as described in section 2.5.

(ix) Once analysis procedure and thresholds were fixed, the search for gravitational wave bursts was applied to the *on-source* data set. The statistical analysis led to confidence intervals which were interpreted as rate upper limit versus amplitude curves. *A posteriori* investigations were performed on the on-source results (see section 3.1), but these follow-up studies did not affect the statistical significance of the *a priori* analysis.

2.1. Accidental coincidences

The statistic of accidental coincidences was studied on independent off-source data sets, obtained with unphysical time shifts between data from the Livingston and Hanford LIGO detectors and AURIGA. The two Hanford detectors were not shifted relative to each other, to account for local Hanford correlated noise. The shifts applied to each LIGO site were randomly chosen between 7 and 100 seconds, with a minimum separation of 1 second between shifts. Hanford-Livingston shifts in the 4-detector search also had to differ by more than 1 second. The livetime in each shifted set varied by a few percents due to the changing combination of data quality cuts in the various detectors. The net live time used in the accidental rate estimate was 2476.4 h from 74 shifts in the four-detector search and 4752.3 h from 67 shifts in the three-detector search.

Figure 3 shows scatter plots of the LIGO Γ versus the AURIGA SNR for background events surviving the cut on the Hanford-Hanford correlation sign, in the 4-detector and in the 3-detector configurations. The regions at SNR < 4.5 and $\Gamma < 4$ are shaded, as they are below the minimal analysis threshold.

The number of off-source accidental coincidences in each time shift should be Poisson distributed if the time slide measurements are independent from each other. For quadruple and for triple coincidences, a χ^2 test compared the measured distributions of the number of accidentals to the Poisson model. The test included accidental coincidences with $\Gamma \geq 4$ and $\Gamma \geq 7.5$ for 4-fold and 3-fold coincidences, respectively. These thresholds were lower than what was used in the coincidence search (sec. 2.3), to ensure a sufficiently large data sample, while the AURIGA threshold remained at SNR ≥ 4.5. The corresponding p-values were 34% and 6.5%, not inconsistent with the Poisson model for the expected number of accidentals.

2.2. Network detection efficiency

The detection efficiency was estimated by adding software-generated signals to real data, according to the LIGO Mock Data Challenge procedure [23]. The simulation generated gravitational waves from sources isotropically distributed in the sky, with azimuthal coordinate uniform in $[0, 2\pi]$, cosine of the polar sky coordinate uniform in $[-1, 1]$ and wave polarization angle uniform in $[0, \pi]$. Three waveform classes were considered [17, 19]:

(i) *Gaussians*:

$$\begin{cases} h_+(t) = h_{peak}\, \mathrm{e}^{-(t-t_0)^2/\tau^2} \\ h_\times(t) = 0 \end{cases}$$

with $\tau = 0.2\,\mathrm{ms}$.

(ii) *sine-Gaussians* and *cosine-Gaussians*:

$$\begin{cases} h_+(t) = h_{peak}\, \mathrm{e}^{-(t-t_0)^2/\tau^2}\, \sin(2\pi f_0(t-t_0)) \\ h_\times(t) = 0 \end{cases}$$

with $f_0 = 900\,\mathrm{Hz}$, $\tau = 2/f_0 = 2.2\,\mathrm{ms}$ and $Q \equiv \sqrt{2}\pi f_0 \tau = 8.9$. In this analysis we found the same results for sine-Gaussians and cosine-Gaussian waveforms.

(iii) *Damped sinusoids*:

$$h_+(t) = \begin{cases} h_{peak}\, \dfrac{1+\cos^2\iota}{2}\, \cos[2\pi f_0(t-t_0)]\, \mathrm{e}^{-(t-t_0)/\tau} & t-t_0 \geq 0\,, \\ h_{peak}\, \dfrac{1+\cos^2\iota}{2}\, \cos[2\pi f_0(t-t_0)]\, \mathrm{e}^{10(t-t_0)/\tau} & t-t_0 < 0\,, \end{cases}$$

$$h_\times(t) = \begin{cases} h_{peak}\, \cos\iota\, \sin[2\pi f_0(t-t_0)]\, \mathrm{e}^{-(t-t_0)/\tau} & t-t_0 \geq 0 \\ h_{peak}\, \cos\iota\, \sin[2\pi f_0(t-t_0)]\, \mathrm{e}^{10(t-t_0)/\tau} & t-t_0 < 0 \end{cases}$$

with $f_0 = 930\,\mathrm{Hz}$, $\tau = 6\,\mathrm{ms}$ and $cos\iota$ uniformly distributed in $[-1, 1]$, ι being the inclination of the source with respect to the line of sight.

Although no known astrophysical source is associated with Gaussian and sine-Gaussian waveforms, they are useful because of their simple spectral interpretation and they are standard test waveforms in LIGO burst searches. Damped sinusoids are closer to physical templates [2, 15, 16].

The signal generation was performed by the LIGO software `LDAS` [25]; the waveforms were added to calibrated LIGO and AURIGA data and the result was analyzed by the same pipeline used in the search. For each waveform class, the simulation was repeated at different signal amplitudes to measure the efficiency of the network as a function of the square root of the burst energy:

$$h_{rss} = \sqrt{\int_{-\infty}^{\infty} dt\, \left[h_+^2(t) + h_\times^2(t)\right]} = \sqrt{2\int_0^{\infty} df\, \left[\tilde{h}_+^2(f) + \tilde{h}_\times^2(f)\right]}.$$

Figure 4 shows scatter plots of the LIGO Γ versus the AURIGA SNR in the 4-fold analysis, for linearly polarized sine-Gaussian simulated waveforms and for circularly polarized damped sinusoids with $|\cos\iota| > 0.966$. For linearly polarized signals, the scatter plot has no structure, due to the different antenna patterns affecting the signal amplitude at the detectors. The effect of misalignment is mitigated in the case of circularly polarized waveforms, where a correlation between the LIGO and AURIGA measures can be noticed in the scatter plots.

2.3. Analysis tuning

The analysis thresholds were chosen to maximize the detection efficiency with an expected number of accidental coincidences smaller than 0.1 in each of the three and the four detector searches. Figure 5 shows contour plots of the number of accidental coincidences expected in the on-source data set, the original un-shifted data that may include a gravitational wave signal, as a function of the Γ and SNR thresholds. This quantity is the number of accidental coincidences found in in the time shifted data, scaled by the ratio of on-source to off-source livetimes. The plots also show the detectability of sine-Gaussian waveforms, expressed as $h_{rss}50\%$, the signal amplitude with 50% detection probability.

For all tested waveforms, the detection efficiency in the 4-fold and 3-fold searches are the same, within 10%; their value is dominated by the AURIGA sensitivity at

SNR $\geq$ 4.5. This observation, together with the shape of the accidental rate contour plots, indicates that the best strategy for the suppression of accidental coincidences with minimal impact on detection efficiency is to increase the Γ threshold and leave the SNR threshold at the exchange value of 4.5. The analysis thresholds were chosen to yield the same accidental rate in the two data sets: $\Gamma \geq 6$ and SNR $\geq$ 4.5 for the 4-fold search and $\Gamma \geq 9$ and SNR $\geq$ 4.5 for the 3-fold search.

It was decided *a priori* to quote a single result for the entire observation time by merging the 4-fold and the 3-fold periods. The number of expected accidental coincidences in the combined on-source data set is 0.24 events in 110.0 hours, with a 1σ statistical uncertainty of 0.06. Detection efficiencies with the chosen thresholds are listed in table 1.

Waveform	$h_{rss}50\%$ $[10^{-20}\mathrm{Hz}^{-1/2}]$		$h_{rss}90\%$ $[10^{-19}\mathrm{Hz}^{-1/2}]$	
	4-fold	3-fold	4-fold	3-fold
sine-Gaussians	5.6	5.8	4.9	5.3
Gaussians	15	15	10	11
damped sinusoids	5.7	5.7	3.3	3.4

Table 1. Signal amplitudes with 50% and 90% detection efficiency in the 4-fold and 3-fold searches at the chosen analysis thresholds of SNR $\geq$ 4.5 and $\Gamma \geq 6$ (4-fold) or $\Gamma \geq 9$ (3-fold). These numbers are affected by a $\sim$ 10% systematic error, due to calibration uncertainties, and a $\sim$ 3% 1σ statistical error, due to the small number of simulated signals.

2.4. Error propagation

The detection efficiency, in a coincidence analysis, is dominated by the least sensitive detector, in this case AURIGA. The Montecarlo efficiency studies also lost a small fraction of the simulated events due to LIGO. However, the exact value of the Γ threshold and the LIGO calibration uncertainty were not the main cause; these events were missed because because their sky-location and polarization were in an unfavorable part of LIGO's antenna pattern. The main source of systematics in this analysis is thus the calibration error on AURIGA, estimated to be $\sim$ 10%.

In addition, there is a statistical error due to the simulation statistics and to the uncertainty on the asymptotic number of injections after the veto implementation. The 1σ statistical error on the numbers in table 1 is about 3%.

Both systematic and statistical errors were taken into account in the final exclusion curve in figure 8. The systematic error is propagated from the fit of the efficiency curve to a 4-parameter sigmoid (see [7, 8, 9] for details). The fit parameters were worsened to ensure a 90% confidence level in the fit, following the prescriptions in [28]. An additional, conservative shift to the left was applied to account for the 10% error on the calibration uncertainty (which is the dominant error).

2.5. Statistical interpretation plan

In compliance with the blind analysis approach, the statistical interpretation was established *a priori*. The procedure is based on a null hypothesis test to verify that the number of on-source coincidences is consistent with the expected distribution of

accidentals, a Poisson with mean 0.24. We require a 99% test significance, which implies the null hypothesis is rejected if at least 3 coincidences are found.

The set of alternative hypotheses is modeled by a Poisson distribution:

$$P(n|\mu) = (\mu + b)^n \exp[-(\mu + b)]/n! \tag{1}$$

where the unknown μ is the mean number of counts in excess of the accidental coincidences, which could be due to gravitational waves, to environmental couplings or to instrumental artifacts. Confidence intervals are established by the Feldman and Cousins method with 90% coverage [26]. Uncertainties on the estimated accidental coincidence number are accounted for by taking the union of the two confidence belts with $b = 0.24 \pm 3\sigma$, with $\sigma = 0.06$.

The confidence belt was modified to control the false alarm probability according to the prescription of the null hypothesis test: if less than 3 events are found, and the null hypothesis is confirmed at 99% C.L., we accept the upper bound of the Feldman and Cousins construction but we extend its lower bound to 0 regardless of the belt value. The resulting confidence belt, shown in figure 6, is slightly more conservative than the standard Feldman and Cousins' for small values of the signal μ. The advantage of this modification is to separate the questions of what is an acceptable false detection probability and what is the required minimum coverage of the confidence intervals [27].

An excess of on-source coincidences could be due to various sources, including instrumental and environmental correlations; the rejection of the null hypothesis or a confidence interval on μ detaching from zero do not automatically imply a gravitational wave detection. A detection claim requires careful follow-up studies, to rule out all known sources of foreground, or an independent evidence to support the astrophysical origin of the signal. On the other hand, an upper limit on μ can be interpreted as an upper limit on the number of GWs.

Only the upper bound of the confidence interval is used to construct the exclusion curves in Fig. 8.

3. Results

The final step consists of analyzing the on-source data sets. No gravitational-wave candidates were found in this search, consistent with the null hypothesis. The resulting 90% CL upper limit is 2.4 events in the on-source data set, or 0.52 events/day in the combined 3-fold and 4-fold data sets.

Figure 7 shows the combined efficiency for this search as a function of the signal amplitude for the waveforms described in section 2.2, a weighted average of the detection efficiency of 3-fold and 4-fold searches:

$$\varepsilon(\mathrm{h_{rss}})_{\mathrm{4fold+3fold}} = \frac{\varepsilon(\mathrm{h_{rss}})_{\mathrm{4fold}} \cdot \mathrm{T_{4fold}} + \varepsilon(\mathrm{h_{rss}})_{\mathrm{3fold}} \cdot \mathrm{T_{3fold}}}{\mathrm{T_{4fold}} + \mathrm{T_{3fold}}} \tag{2}$$

The 90% C.L. rate upper limit, divided by the amplitude-dependent efficiency, yields upper limit exclusion curves similar to those obtained in previous searches [7, 11]. Figure 8 compares the sine-Gaussian exclusion curves found in this search to those from S2 in LIGO and LIGO-TAMA. The waveform used here peaks at 900 Hz, while the previous searches used a sine-Gaussian with 850 Hz central frequency. We verified analytically that the AURIGA detection efficiencies for sine-Gaussians Q=9 at 850 Hz and 900 Hz agree within 10%; no difference is to be expected for the large band detectors.

The asymptotic upper limit for large amplitude signals is inversely proportional to the observation time. The value for this search with 90% C.L. is 0.51 events/day, to be compared to 0.26 events/day in the LIGO S2 search [7] and 0.12 events/day in the LIGO-TAMA search [11]. The lowest asymptotic value was previously set by IGEC: $\sim 4 \times 10^{-3}$events/day, thanks to the longer observation time [4].

The detection efficiency in this search is comparable to the LIGO-only S2 one, and a factor 2 worse than the LIGO-only S3. In the lower amplitude region, this search is an improvement over the IGEC search, since the AURIGA amplitude sensitivity during LIGO S3 was about 3 times better than the typical bar sensitivity in the IGEC 1997-2000 campaign (a direct comparison is not possible since IGEC results are not interpreted in terms of a source population model). More recent data yielded significant improvements in sensitivities, by a factor ~ 10 for the LIGO S4 run [9] and a factor ~ 3 for IGEC-2 [5].

3.1. Diagnostics of on-source and off-source data sets

The agreement between on-source and off-source coincidences was tested comparing the Γ distributions in Figure 9 above the minimal exchange threshold $\Gamma \geq 4$ and below the network analysis threshold ($\Gamma \geq 6$ for 4-fold and $\Gamma \geq 9$ for 3-fold). This *a posteriori* test did not find a disagreement between on-source and off-source distributions. There were no 4-fold, on-source events with $\Gamma \geq 4$. For 3-fold events, the agreement between zero-lag and accidental distributions can be confirmed with a Kolmogorov-Smirnov test that uses the empirical distribution of accidentals as a model, with a 0.6 p-value.

In addition, we addressed the question of whether on-source events (foreground) modified the distribution of accidentals (background) and biased our estimate. This is an issue in the 3-fold AU-H1-H2 analysis where only H1 and H2 are cross-correlated and the measured background distribution includes instances of Hanford foreground events in accidental coincidence with an AURIGA shifted event. As a result, the time shift method overestimates the number of accidentals. In this search, however, this systematic effect turned out being negligible: once we removed all background events in accidental coincidence with on-source 3-fold events with $\Gamma \geq 5.5$ and SNR ≥ 4.5, the resulting histogram was not significantly affected, as shown in Figure 10.

The same question could be posed in a different way around: how would the background histogram change if we had an actual gravitational wave events, with large Γ? On average, the same loud H1-H2 event appears in ~ 9 background coincidences. Consequently, an actual gravitational wave with Γ above the noise, say $\Gamma = 12$, would have appeared on the background histogram 15-20 times as a Γ peak with a tail at the same Hanford time. Such an event would not have been missed, but it would have been noticed in the tuning stages. The most significant consequence is that the 3-fold search is not truly blind, since a loud signal would easily manifest itself in the tuning data set.

4. Conclusions

This paper describes the first joint search for gravitational wave bursts with a hybrid network composed of a narrow band resonant bar detector and broadband interferometers. This was a precious opportunity to bring together the expertise of the AURIGA and LSC collaborations and explore common methods on real data. The addition of the AURIGA detector to the LIGO observatory allowed to extend the

time coverage of the observations by including also the time periods when only two of the three LIGO detectors were operating simultaneously with AURIGA. This has been possible thanks to the suppression in false alarm rate contributed by AURIGA (AU-H1-H2). At the same time, the detection efficiency of this hybrid network for the tested source models was about a factor 2 worse than the LIGO-only efficiency, being dominated by the AURIGA detector. This cost however, turned out to be smaller than the 3:1 amplitude sensitivity ratio between AURIGA and LIGO during S3 for the same signal types.

Due to the short observation time, the relevance of this study is methodological. The results have been interpreted in terms of source population models and the final upper limits are comparable to those set by LIGO only in previous observations. This joint analysis followed a statistically *blind* procedure to allow an unbiased interpretation of the confidence of the results. In particular, the data analysis plan has been fixed *a priori* and the results are confidence intervals which ensure a minimum coverage together with a more stringent requirement on the maximum false detection probability.

Further joint searches for bursts by interferometric and resonant detectors are nowadays possible exploiting simultaneous long term observations and we are considering the opportunities of such future collaborations.

Acknowledgments

The LIGO Scientific Collaboration (LSC) gratefully acknowledges the support of the United States National Science Foundation for the construction and operation of the LIGO Laboratory and the Particle Physics and Astronomy Research Council of the United Kingdom, the Max-Planck-Society and the State of Niedersachsen/Germany for support of the construction and operation of the GEO600 detector. The authors also gratefully acknowledge the support of the research by these agencies and by the Australian Research Council, the Natural Sciences and Engineering Research Council of Canada, the Council of Scientific and Industrial Research of India, the Department of Science and Technology of India, the Spanish Ministerio de Educacion y Ciencia, The National Aeronautics and Space Administration, the John Simon Guggenheim Foundation, the Alexander von Humboldt Foundation, the Leverhulme Trust, the David and Lucile Packard Foundation, the Research Corporation, and the Alfred P. Sloan Foundation.

The AURIGA Collaboration acknowledges the support of the research by the Istituto Nazionale di Fisica Nucleare (INFN), the Universities of Ferrara, Firenze, Padova and Trento, the Center of Trento of the Istituto di Fotonica e Nanotecnologie - Istituto Trentino di Cultura and the Consorzio Criospazio Ricerche of Trento.

References

[1] Ott C D, Burrows A, Dessart L, and Livne E (2006) Phys. Rev. Lett. **96**, 201102

[2] Flanagan É E and Hughes S A (1998) *Measuring gravitational waves from binary black hole coalescences. I. Signal to noise for inspiral, merger, and ringdown*, Phys. Rev. D **57**, 4535.

[3] Flanagan É E and Hughes S A (1998), Phys. Rev. D **57**, 4566.

[4] Astone P et al. (2003) *Methods and results of the IGEC search for burst gravitational waves in the years 1997-2000*, Phys. Rev. D **68**, 022001.

[5] Astone P et al. *Results of the IGEC-2 search for gravitational wave bursts during 2005*, submitted to Phys Rev D

[6] Abbott B et al. (LIGO Scientific Collaboration) (2004) *First upper limits from LIGO on gravitational-wave bursts*, Phys. Rev. D **69**, 102001.

[7] Abbott B et al. (LIGO Scientific Collaboration) (2005) *Upper limits on gravitational wave bursts in LIGO's second science run*, Phys. Rev. D **72**, 062001.

[8] Abbott B et al. (LIGO Scientific Collaboration) (2006) *Search for gravitational-wave bursts in LIGO's third science run.*, Class. Quant. Grav. **23**, S29-S39

[9] Abbott B et al. (LIGO Scientific Collaboration) *earch for gravitational-wave bursts in LIGO data from the fourth LSC science run.*, preprint arXiv:0704.0943, submitted Class. Quant. Grav.

[10] Ando M et al. (2005) *Observation results by the TAMA300 detector on gravitational wave bursts from stellar-core collapses*, Phys. Rev. D **69**, 082002.

[11] Abbott B et al. (2005) *Upper limits from the LIGO and TAMA detectors on the rate of gravitational-wave bursts*, Phys. Rev. D **72**, 122004.

[12] Zendri J P et al (2003) *Status report of the gravitational wave detector AURIGA*, in "Gravitational Waves and Experimental gravitation", proceeding of the "XXXVIIIth Moriond Workshop", Dumarchez and J. Tran Thanh Van, The Gioi Publishers, Vietnam, 37-42.

[13] Vinante A (for the AURIGA Collaboration), (2006), *Present performance and future upgrades of the AURIGA capacitive readout*, Class. Quantum Grav. **23** S103-S110

[14] Baggio L et al. (2005) *3-mode detection for widening the bandwidth of resonant gravitational wave detectors*, Phys. Rev. Lett. **94**, 241101.

[15] Baker J et al. (2002) *Modeling gravitational radiation from coalescing binary black holes*, Phys. Rev. D **65**, 124012.

[16] Campanelli M, Lousto C O, and Zlochower Y *Last orbit of binary black holes* Phys. Rev. D **73**, 061501 (2006)

[17] Poggi S (2006)*A joint search for gravitational wave bursts by the AURIGA resonant detector and the LIGO interferometer observatories*, PhD thesis, Università degli Studi di Trento, Italy. Available online at: http://www.auriga.lnl.infn.it/auriga/papers_src/phd_poggi.zip

[18] Cadonati L et al. 2005 *The AURIGA-LIGO Joint Burst Search*, Class. Quantum Grav. **22**, S1337-S1347.

[19] Poggi S and Salemi F (for the AURIGA collaboration) and Cadonati L (for the LIGO Scientific collaboration) (2006) *Status of the LIGO-AURIGA Joint Burst Search* Journal of Physics: Conference Series **32**, 198-205.

[20] Cadonati L (2004) *Coherent waveform consistency test for LIGO burst candidates.*, Class. Quantum Grav. **21**, S1695-S1703.

[21] Cadonati L and Márka S (2005) *CorrPower: a cross-correlation-based algorithm for triggered and untriggered gravitational-wave burst searches*, Class. Quantum Grav. **22**, S1159-S1167.

[22] Finn L S (2003) *S3 Playground Selection*, LIGO-T030256-00-Z, LIGO internal report

[23] Yakushin I, Klimenko S and Rakhmanov M (2004) *MDC frames for S2 burst analysis*, LIGO-T040042-00-Z-00 D, LIGO internal report available in the LIGO Document Control Center at www.ligo.caltech.edu/docs/T/T040042-00.pdf

[24] Katsavounidis E (2005), *Searches for gravitational-wave bursts with LIGO*, Slides of the talk for the "Sixth Edoardo Amaldi Conference" in: http://tamago.mtk.nao.ac.jp/amaldi6/07.da2/Thu1125_bwg-amaldi6-v3.ppt

[25] The LIGO Data Analysis System home page is http://www.ldas-sw.ligo.caltech.edu

[26] Feldman G J and Cousins R D (1998) *Unified approach to the classical statistical analysis of small signals*, Phys. Rev. D **57**, 3873-3889.

[27] see Baggio L and Prodi G A, *Statistical problems associated with the analysis of data from a network of narrow-band detectors, in Statistics for Gravitational Wave Data Analysis*, Center for Gravitational Wave Physics, Penn State University, 19-21 May 2005, http://cgwp.gravity.psu.edu/events/GravStat/Prodi_GravStat.ppt

[28] F. James, "MINUIT: Function Minimization and Error Analysis" Reference Manual, Version

94.1 (1994) CERN document D506

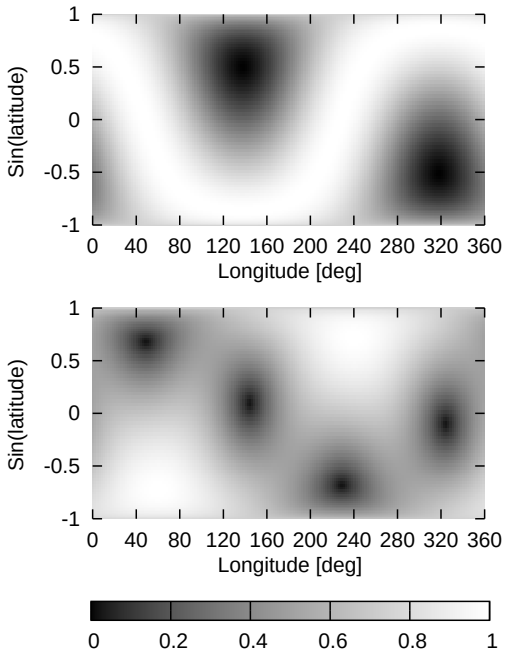

Figure 1. Antenna pattern magnitude as a function of the longitude and the sine of the latitude. Top: AURIGA; bottom: LIGO-Hanford.

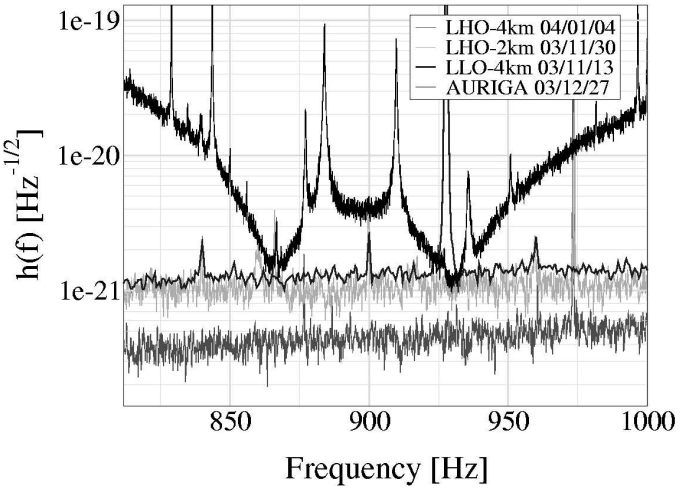

Figure 2. Best single-sided sensitivity spectra of AURIGA and the three LIGO interferometers during the joint observation. In the AURIGA spectrum, several spurious lines are visible while LIGO spectra present calibration lines at 973 Hz for the Hanford detectors (LHO-4 km and LHO-2 km) and 927 Hz for the Livingston detector (LLO-4 km).

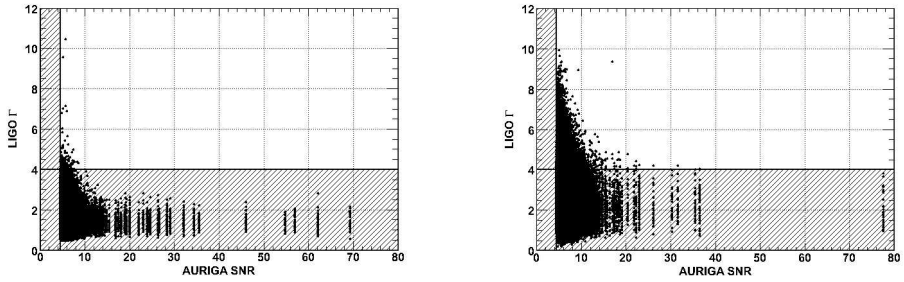

Figure 3. Scatter plots of the LIGO Γ versus the AURIGA SNR for background events surviving the cut on the sign of the H1-H2 correlation, in the 4-detector (left) and in the 3-detector (right) configurations. The regions at SNR < 4.5 and $\Gamma < 4$ are shaded, as they are below the minimal analysis threshold and were not used in the tuning.

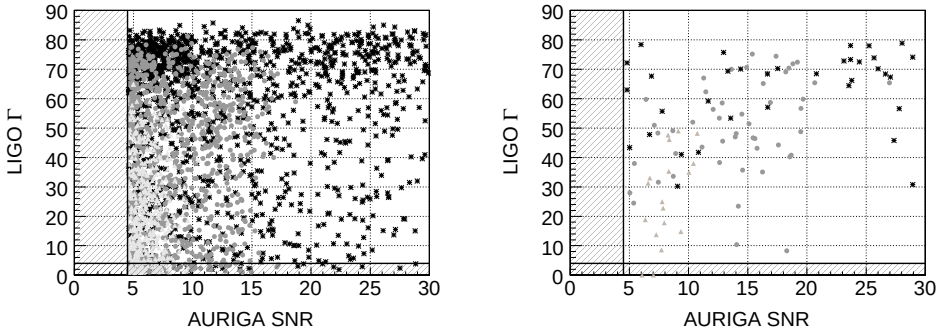

Figure 4. Scatter plots of the LIGO Γ versus the AURIGA SNR for simulated signals in 4-fold coincidence, with three amplitudes: $h_{rss} = 1.2 \times 10^{-19}\mathrm{Hz}^{-1/2}$ (stars), $h_{rss} = 6 \times 10^{-20}\mathrm{Hz}^{-1/2}$ (circles) and $h_{rss} = 3 \times 10^{-20}\mathrm{Hz}^{-1/2}$ (triangles).

Left: linearly polarized sine-Gaussians waveforms, in general seen with different amplitudes by LIGO and AURIGA, thus the scatter plot has no structure.

Right: damped sinusoids, circularly polarized, and $|\cos\iota| > 0.966$ (see equation 1). In this case, the misalignment effect is mitigated and a correlation can be seen between the LIGO and AURIGA measures. Outliers correspond to unfavorable antenna patterns.

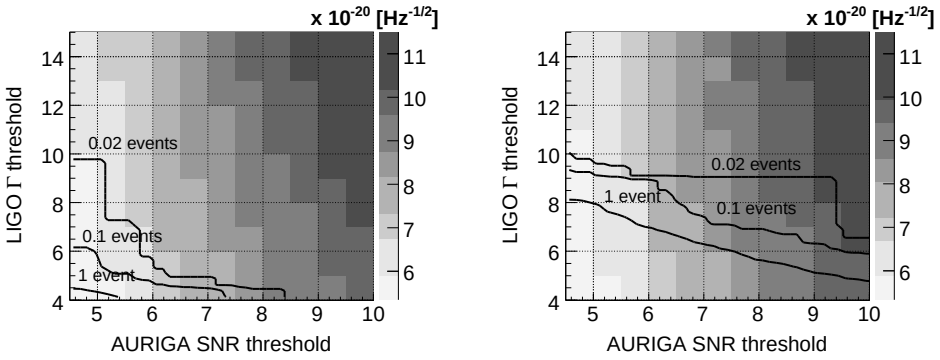

Figure 5. Gray scale plot: efficiency to sine-Gaussians waveforms and false alarms in terms of $h_{rss}50\%$. Left: 4-fold; right: 3-fold observations.
The contour lines indicate the number of accidental coincidences expected in the on-source data set.

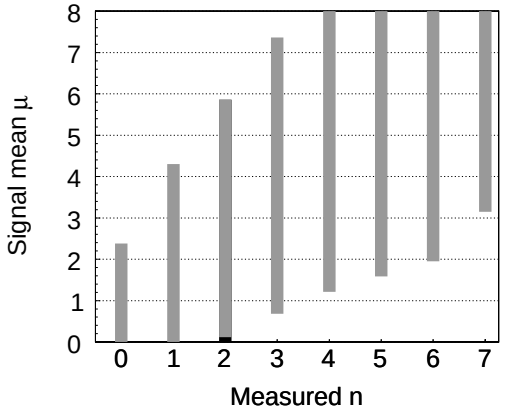

Figure 6. Confidence belt based on the Feldman and Cousins's procedure, with 90% C.L., unknown Poisson signal mean μ and a Poisson background with $b = 0.24 \pm 3\sigma$. The standard Feldman and Cousins construction (solid lines) is modified by fixing the maximum false alarm probability to 1%: the lower bound is fixed to 0 for 2 measured events.

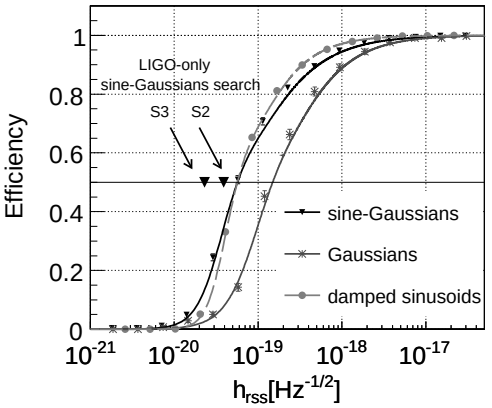

Figure 7. Average efficiency of detection (4-fold+3-fold) versus h_{rss} for the considered waveforms: sine-Gaussians at $f_0 = 900$ Hz and $\tau = 2.2$ ms, Gaussians with $\tau = 0.2$ ms, and damped sinusoids with $f_0 = 930$ Hz and damping time $\tau = 6$ ms. All sources have been modelled as uniformly distributed in the sky and with random polarizations (see section 2.2). The triangle marks the $h_{rss}50\% = 2.3 \times 10^{-20}\mathrm{Hz}^{-1/2}$ achieved by LIGO-only during S3 for sine-Gaussians.

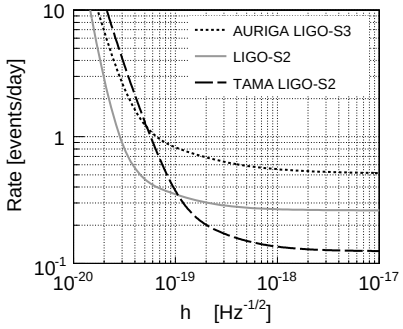

Figure 8. Upper limits at 90% C.L. on the gravitational wave rate versus h_{rss} for sine-Gaussian waveforms in different network analyses: AURIGA-LIGO S3 (dotted line), LIGO-only S2 (continue line) and TAMA-LIGO S2 (dashed line). The sine-Gaussians have central frequency 900 Hz (for AURIGA-LIGO S3) and 850 Hz (for LIGO-only S2 and TAMA-LIGO S2). In all cases, $Q = 8.9$. All sources have been modelled as uniformly distributed in the sky and with random polarizations (see section 2.2)

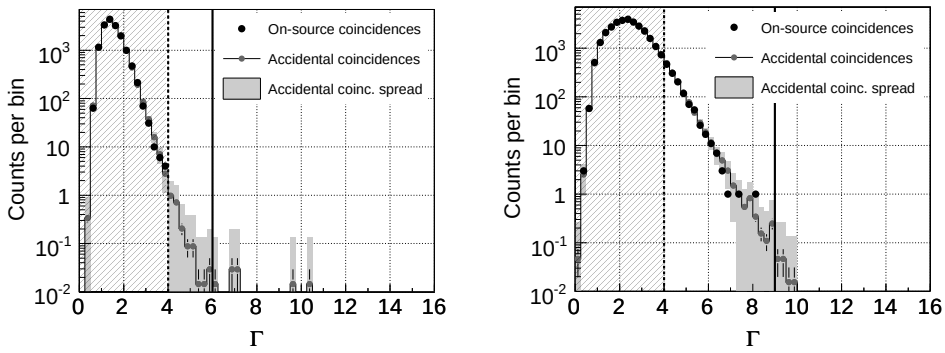

Figure 9. Comparison of Γ distributions for four-fold (left) and three-fold coincidences (right). The black dots correspond to on-source coincidences. The stair-step curve with gray dots is the mean accidental contribution, estimated from off-source coincidences, with its 1σ RMS spread (gray bars). The on-source and off-source distributions are in good agreement, within the statistical uncertainty. The smaller gray error bars are the error on the mean contribution of the accidental coincidences. The solid vertical lines correspond to the analysis thresholds ($\Gamma = 6$ and $\Gamma = 9$, respectively). The analysis was tuned only on events with $\Gamma \geq 4$ (dotted vertical lines).

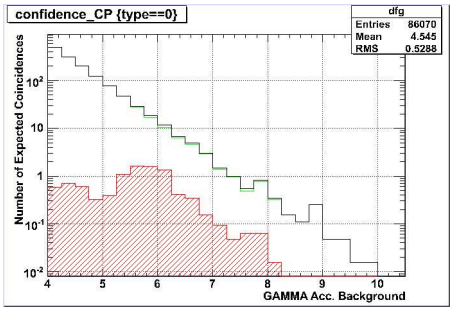

Figure 10. Γ histogram of off-source events in the 3-fold AU-H1-H2 analysis, normalized to the on-source livetime. Solid line: all. Dashed line: overlap of on-source and off-source event sets (background events that overlap with on-source events with $\Gamma \geq 5.5$ and $SNR \geq 4.5$). Dotted line: difference of the two. Placeholder for a better figure